Node-dependent kinematic elements for the dynamic analysis of beams with piezo-patches

Node-Dependent Kinematic Elements for the Dynamic Analysis of Beams with Piezo-patches

Journal of Intelligent Material Systems and Structures
XX(X):1–15

DOI: 10.1177/ToBeAssigned
www.sagepub.com/
SAGE

Enrico Zappino[1], Guohong Li[1] and Erasmo Carrera[1]

Abstract

This paper extends the use of one-dimensional elements with node-dependent kinematics (NDK) to the dynamic analysis of beam structures with piezo-patches. NDK allows the kinematic assumptions to be defined individually on each finite element (FE) node, leading to FE models with variable nodal kinematics. Derived from Carrera Unified Formulation (CUF), NDK facilitates the mathematical refinement to an arbitrary order at any desirable region on the nodal level while keeping the compactness of the formulation. As an ideal approach to simulate structures with special local features, NDK has been employed to model piezo-patches in static cases. In the present work, the application of ND beam elements in dynamic problems is demonstrated. NDK is applied to increase the numerical accuracy in the areas where the piezo-patches lie in through sufficiently refined models, while lower order assumptions are used elsewhere. The dissimilar constitutive relations of neighboring components are appropriately considered with layer-wise (LW) models. Both open and short circuit conditions are considered. The results are compared against those from literature. The numerical study shows that the adoption of NDK allows accurate results to be obtained at reduced computational costs.

Keywords

Beam element, Carrera Unified Formulation, Piezo-patch, Node-dependent kinematics, dynamic analysis

Introduction

Piezoelectric components have draw significant attention as vibration control devices. Effective modeling techniques should address the different constitutive relations in different regions, the electromechanical coupling effect, and the segmented distribution of piezo-patches.

By considering the electric potential as a primary variable in the formulation, the electromechanical coupling can be captured, and both sensor and actuator cases can be modeled. A great variety of FE modeling techniques have been put forward for the modeling of piezoelectric devices, including 1D, 2D and 3D elements by category. 3D brick elements for piezoelectric modeling were presented by Allik and Hughes (1970), and Batra and Liang (1997). Since solid elements are computational costly when used to model thin piezoelectric layers, various 2D and 1D models were proposed as alternative choices. Early models include those based on the Classical Lamination Theory (CLT) as presented by Lee (1990) and Wang and Rogers (1991), or First-Order Shear Deformation Theory (FSDT) such as Huang and Wu (1996), Jonnalagadda et al. (1994), and Batra (1995). For these classical models, the stress and electric displacement variation through the thickness

[1] MUL^2 group, Department of Mechanical and Aerospace Engineering, Politecnico di Torino

Corresponding author:
E. Zappino, Department of Mechanical and Aerospace Engineering Politecnico di Torino, Corso Duca degli Abruzzi 24, 10129 Torino, Italy.
Email: enrico.zappino@polito.it

cannot be well captured. Improvement can be achieved by adopting Higher-Order Theory (HOT) (Mitchell and Reddy 1995). By extending a zig-zag theory for laminated plates to the electromechanical case (Kapuria 2001, 2004), the interlaminar continuity can be better considered. Alternatively, the electric displacement components and the transverse shear stresses can be better approximated through layer-wisely defined approximation functions in the thickness domain, as discussed by Heyliger et al. (1994). In a similar approach, refined layer-wise (LW) beam elements were also developed by Robbins and Reddy (1991). In fact, LW models can help to facilitate materials with different constitutive in neighboring layers. To reduce the computational costs, Kim et al. (1997) developed transition elements to connect 2D elements for pure structural modeling to 3D elements used to model the piezoelectric devices. For more detailed reviews on the modeling techniques of structures with piezoelectric components, the reader is referred to Benjeddou (2000), Mackerle (2003), and Kapuria et al. (2010). Specially, Benjeddou (2000) and Chevallier et al. (2008) pointed out that a drawback of some piezoelectric FE formulations is the lack of equipotential (EP) constraint for open-circuit static sensing and vibration problems. Whereas, the EP constraint is important for the modeling and understanding of the behaviors of the smart structures (Benjeddou 2000; Trindade and Benjeddou 2009).

Carrera (2002) proposed Unified Formulation (CUF) as a powerful method to build refined 1D and 2D models, in either LW (Carrera and Petrolo 2012) or Equivalent Single Layer (ESL) (Carrera et al. 2010) framework. In CUF, through the *fundamental nuclei* (FNs), the governing equations can be derived in a compact manner, as explicated by Carrera et al. (2014) and Carrera et al. (2016). A variety of CUF-based refined models have been applied to the modeling of smart structures as presented by Carrera et al. (2011) and Cinefra et al. (2015). In addition, Miglioretti et al. (2014) and Zappino et al. (2016a) discussed refined electromechanical beam FE models with variable kinematics. Such type of refined beam elements can provide 3D modeling accuracy at significantly reduced computational costs.

CUF also provides the convenience of defining *nodal kinematics* by relating the mathematical assumption to the chosen FE nodes, leading to a technique known as node-dependent kinematics (NDK). Suggested by Carrera and Zappino (2017), NDK has been applied successfully in the simulation of laminated structures with local effects by Carrera et al. (2018), Zappino et al. (2017), and Carrera et al. (2017a). NDK supports the kinematic refinement at any desirable nodes without using any additional coupling or special transition elements. This technique has been employed to simulate structures with segmented piezo-patches by Carrera et al. (2017b), in which the FE models with variable nodal LW/ESL capabilities were demonstrated to be numerically efficient. As an extension to the authors' previous work (Carrera et al. 2017c) where the static response was investigated, in the present article, the modal property extraction is discussed. Refined beam elements with NDK are applied at the natural frequency analysis of slender structures with piezo-patches. The refined structural models used in the present work have been assessed in the past (Carrera et al. 2012; Zappino et al. 2016b) and their accuracy is not discussed here, but refined models with constant kinematic have been used as reference for the NDK models. The present work aims to show how the use of NDK elements for the modeling of piezo-patched devices may lead to a strong reduction of the computational costs ensuring the same accuracy. This results can be achieved using refined beam models only in those areas where they are required while classical models are used elsewhere.

Node-dependent kinematic beam elements

This section presents a refined one-dimensional finite element model with node-dependent kinematics. In such a model, the kinematic assumptions can be different from node to node in the beam element. For instance, in a 2-node beam element (B2), the Timoshenko theory could be used for node 1, and the Euler-Bernoulli beam theory could be employed on node 2. This approach was firstly introduced by Carrera and Zappino (2017) and are here applied to the dynamic analysis of beam structures with piezo-patches. In

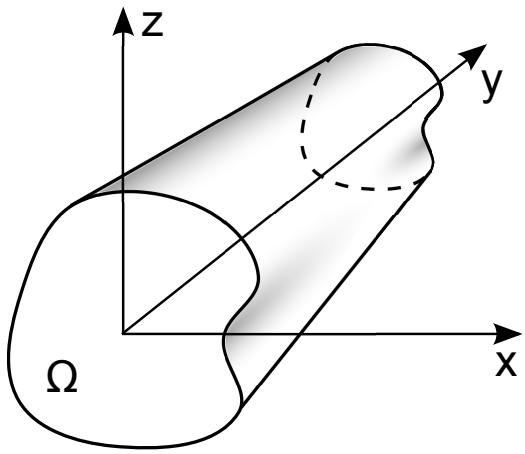

Figure 1. Reference system of the beam model.

the following sections, a brief overview of the refined one-dimensional models is given, and the NDK elements are introduced.

Preliminaries

Figure 1 shows a reference system used to describe a beam model, in which the axial direction is aligned along the y axis. Considering the coupling between electric and mechanical fields, by treating the electric potential ϕ as a primary variable, a generalized displacement vector $\boldsymbol{q}$ can be used:

$$\boldsymbol{q} = \{u_x, u_y, u_z, \phi\}^T \tag{1}$$

and the electric field vector $\boldsymbol{E}$ can be derived from the electric potential ϕ through:

$$\boldsymbol{E} = \{E_x, E_y, E_z\}^T = \{\partial_x, \partial_y, \partial_z\}^T \phi \tag{2}$$

The generalized strain vector, $\bar{\varepsilon}$, can be written as:

$$\bar{\boldsymbol{\varepsilon}} = \{\varepsilon_{xx}, \varepsilon_{yy}, \varepsilon_{zz}, \varepsilon_{xz}, \varepsilon_{yz}, \varepsilon_{xy}, E_x, E_y, E_z\}^T = \boldsymbol{D}\boldsymbol{q} \tag{3}$$

where the differential operator matrix $\boldsymbol{D}$ is:

$$\boldsymbol{D} = \begin{bmatrix} \frac{\partial}{\partial x} & 0 & 0 & 0 \\ 0 & \frac{\partial}{\partial y} & 0 & 0 \\ 0 & 0 & \frac{\partial}{\partial z} & 0 \\ \frac{\partial}{\partial z} & 0 & \frac{\partial}{\partial x} & 0 \\ 0 & \frac{\partial}{\partial z} & \frac{\partial}{\partial y} & 0 \\ \frac{\partial}{\partial y} & \frac{\partial}{\partial x} & 0 & 0 \\ 0 & 0 & 0 & \frac{\partial}{\partial x} \\ 0 & 0 & 0 & \frac{\partial}{\partial y} \\ 0 & 0 & 0 & \frac{\partial}{\partial z} \end{bmatrix} \tag{4}$$

The electromechanical constitutive equations (*e-form*) can be expressed as follows:

$$\begin{aligned} \boldsymbol{\sigma} &= \tilde{\boldsymbol{C}}\boldsymbol{\varepsilon} - \tilde{\boldsymbol{e}}^T \boldsymbol{E} \\ \boldsymbol{D}_e &= \tilde{\boldsymbol{e}}\boldsymbol{\varepsilon} + \tilde{\boldsymbol{\chi}}^T \boldsymbol{E} \end{aligned} \tag{5}$$

in which $\boldsymbol{D}_e$ is the electric displacement vector $\{D_x, D_y, D_z\}^T$, and $\boldsymbol{\sigma}$ is the mechanical stress vector, $\tilde{\boldsymbol{C}}$ the matrix of mechanical material coefficients. The dielectric permittivity matrix $\tilde{\boldsymbol{\chi}}$ and the piezoelectric stiffness coefficient matrix $\tilde{\boldsymbol{e}}$ are determined by the poling direction and a rotation angle. For more details about the rotation of piezoelectric material coefficient matrices the reader is referred to Kpeky et al. (2017); Benjeddou et al. (1997); Kapuria and Hagedorn (2007).

The generalized stress vector $\bar{\boldsymbol{\sigma}}$ can be arranged as:

$$\bar{\boldsymbol{\sigma}} = \{\sigma_{xx}, \sigma_{yy}, \sigma_{zz}, \sigma_{xz}, \sigma_{yz}, \sigma_{xy}, D_x, D_y, D_z\}^T \tag{6}$$

In a compact form, $\bar{\boldsymbol{\sigma}}$ can be obtained through the following constitutive relation:

$$\bar{\boldsymbol{\sigma}} = \begin{bmatrix} \tilde{\boldsymbol{C}} & -\tilde{\boldsymbol{e}}^T \\ \tilde{\boldsymbol{e}} & \tilde{\boldsymbol{\chi}} \end{bmatrix} \bar{\boldsymbol{\varepsilon}} = \tilde{\boldsymbol{H}}\bar{\boldsymbol{\varepsilon}} \tag{7}$$

where $\tilde{\boldsymbol{H}}$ presets the constitutive relations of the piezoelectric components after rotation.

Classical and refined one-dimensional models

The one-dimensional theory approximate a displacement field over the cross-section with assumed functions. An expansion form can be used to describe the behavior of the beam cross-section. This approach, suggested by Washizu

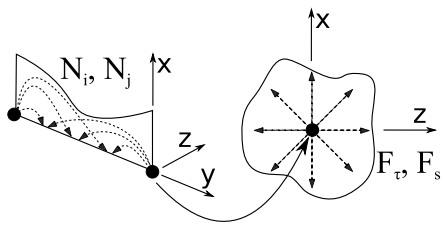

Figure 2. A two-nodes beam with Taylor expansions (TE).

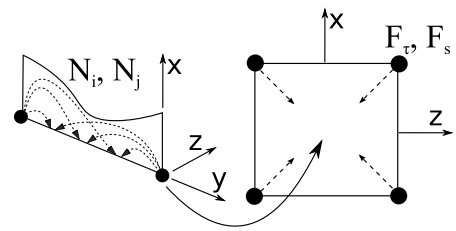

Figure 3. A two-nodes beam based employing Lagrange expansions (LE).

(1968), leads the expression of the three-dimensional displacement field as:

$$\boldsymbol{u} = \boldsymbol{u}_\tau(y) F_\tau(x,z), \qquad \tau = 1 \dots M. \tag{8}$$

where $F_\tau(x,z)$ is the function expansion over the cross-section, and $\boldsymbol{u}_\tau(y)$ is the unknown vector along the beam axis, M the number of terms in the function expansion $F_\tau(x,z)$. Various choices for the approximation functions $F_\tau(x,z)$ can lead to a number of kinematic models. In the present work, Taylor and Lagrange expansions are considered. The solution to the one-dimensional problem reported in Equation 8 can be obtained using the finite element (FE) method, which allows the system of partial derivative functions to be reduced to an algebraic system. FEs approximate the axial unknowns $\boldsymbol{u}_\tau(y)$ by using the one-dimensional shape functions N_i, which lead to the following displacement field assumption:

$$\boldsymbol{u} = N_i(y) F_\tau(x,z) \boldsymbol{u}_{i\tau}, \qquad \tau = 1 \dots M; \qquad i = 1 \dots N_n. \tag{9}$$

where N_i are the shape functions introduced by the FE model, and N_n is the number of nodes in the element, $\boldsymbol{u}_{i\tau}$ the nodal unknowns.

The one-dimensional models based on the Taylor Expansion (TE) approximate the cross-sectional deformation with 2D polynomials $x^m\ z^n$, where m and n are positive integers. Figure 2 shows a representation of a B2 element based on the TE expansions. In this case, the F_τ and F_s functions are used to expand the solution from the beam node to the cross-section. Classical models such as Euler-Bernoulli and Timoshenko can be obtained as particular cases of the TE models.

The case of Euler-Bernoulli, the only one that require a C_1 continuity of the axial shape functions, is obtained through a "downgrade" of the Timoshenko beam model in which a penalty is applied to the shear stiffness.

In the case of models based on the Lagrange Expansions (LE), Lagrange polynomials are applied to build refined one-dimensional models. The iso-parametric formulation is exploited to deal with arbitrarily shaped cross-section geometries. In this paper a quadratic element with nine nodes, LE9, is adopted. When LE is utilized, the unknowns are only the translational displacements of the cross-sectional nodes. Figure 3 illustrates a B2 element adopting LE. The F_τ and F_s functions are used to expand the solution from the cross-sectional nodes to the cross-section area.

A one-dimensional finite element with node-dependent kinematics

When the modeling of structural geometry or boundary conditions is beyond the capabilities of classical beam models, higher-order models can be used to improve the solution precision. Whereas, the refinement of kinematics also increases the computational consumption. In most cases, refined kinematics is necessary only in some local region of the whole structure, e.g. where the assumptions of the classical models are violated, and classical models could be adequate elsewhere. A new class of node-dependent kinematic elements is introduced in this work to refine the kinematics only in the area necessary.

As an example, a three node one-dimensional element is considered. Refined beam elements with uniform kinematics assume the same cross-sectional expansions in all the nodes. By using he node-dependent kinematic approach, a different kinematic assumption can be

introduced at each node. The displacement field at the first node can be written as:

$$\boldsymbol{u}^1 = \boldsymbol{u}_{1\tau} F^1_\tau, \qquad \tau = 1 \dots M^1 \tag{10}$$

The displacement functions at the second node are:

$$\boldsymbol{u}^2 = \boldsymbol{u}_{2\tau} F^2_\tau, \qquad \tau = 1 \dots M^2 \tag{11}$$

Meanwhile, the displacements at the third node read:

$$\boldsymbol{u}^3 = \boldsymbol{u}_{3\tau} F^3_\tau, \qquad \tau = 1 \dots M^3 \tag{12}$$

The cross-sectional expansions, F^1_τ, F^2_τ and F^3_τ, can be chosen arbitrarily at each node. Figure 4 shows a three-node element with node-dependent kinematics. At node 1, a first order TE model has been considered, and a LE model has been imposed at node 2 while a second order TE model is allocated to node 3. Eventually, the expression of the three-dimensional displacement field of the whole element becomes:

$$\boldsymbol{u} = \boldsymbol{u}_{1\tau} N_1 F^1_\tau + \boldsymbol{u}_{2\tau} N_2 F^2_\tau + \boldsymbol{u}_{3\tau} N_3 F^3_\tau, \qquad \tau = 1 \dots M^i \tag{13}$$

The three different displacement fields are smeared by the FE shape functions along the beam length that ensure a smooth transition between the displacement fields of the three nodes. Using this approach, the continuity of the displacement is obtained at each point.

This approach can be easily included in the CUF formulation and extended to any order beam models. The displacement field of the one-dimensional element with node-dependent kinematic can be written including two main novelties:

$$F_\tau(x,z) \longrightarrow F^i_\tau(x,z) \tag{14}$$

$$M \longrightarrow M^i \tag{15}$$

The first equation, Eq. 14, states that the function expansion is not a property of the element, but of the nodes, that is, the index i is included in the notation. Eq. 15 remarks that the number of terms in the expansion, M, can be different at each node, and the notation M^i is used to underline this aspect. The generic displacement field can be written as:

$$\boldsymbol{u} = \boldsymbol{u}_{i\tau} N_i(y) F^i_\tau(x,z), \qquad \tau = 1 \dots M^i; \qquad i = 1 \dots N_n. \tag{16}$$

Governing equations of NDK beam FE models

The governing equations can be derived by applying the principle of virtual displacement (PVD). Consider the energy of the system:

$$\delta L_{int} = \int_V \delta \bar{\boldsymbol{\varepsilon}}^T \bar{\boldsymbol{\sigma}} dV = \delta L_{ext} - \delta L_{ine} \tag{17}$$

where V is the volume of the integration domain, and δL_{int} is the internal energy, δL_{ext} and δL_{ine} the external work and the inertial energy, respectively. For free vibration problems, $\delta L_{ext} = 0$.

By considering the geometrical relations, Equation 3, constitutive equations, Equation 7, as well as the FE discretization, Equation 28, one can obtain:

$$\delta L_{int} = \delta \boldsymbol{q}_{js} \int_V N_j F^j_s \boldsymbol{D}^T \tilde{\boldsymbol{H}} \boldsymbol{D} F^i_\tau N_i dV \boldsymbol{q}_{i\tau} \tag{18}$$

In a compact form, the above expression can be written as:

$$\delta L_{int} = \delta \boldsymbol{q}^T_{js} \boldsymbol{k}_{ij\tau s} \boldsymbol{q}_{i\tau} \tag{19}$$

where $\boldsymbol{k}_{ij\tau s}$ represents the electromechanical *fundamental nuclei* (FNs), which is a core unit of the generalized stiffness matrix:

$$\boldsymbol{k}_{ij\tau s} = \int_V N_j F^j_s \boldsymbol{D}^T \tilde{\boldsymbol{H}} \boldsymbol{D} F^i_\tau N_i dV \tag{20}$$

Actually, $\boldsymbol{k}_{ij\tau s}$ can be further written as:

$$\boldsymbol{k}_{ij\tau s} = \begin{bmatrix} \boldsymbol{k}^{uu} & \boldsymbol{k}^{u\phi} \\ \boldsymbol{k}^{\phi u} & \boldsymbol{k}^{\phi\phi} \end{bmatrix}_{ij\tau s} \tag{21}$$

in which the mechanical stiffness FN $\boldsymbol{k}^{uu}_{ij\tau s}$ is a 3×3 matrix, while the electromechanical coupling FNs $\boldsymbol{k}^{u\phi}_{ij\tau s}$ and $\boldsymbol{k}^{\phi u}_{ij\tau s}$ are 3×1 and 1×3, respectively. The dimension of the pure electric part $\boldsymbol{k}^{\phi\phi}_{ij\tau s}$ is 1×1.

Meanwhile, the inertial work is:

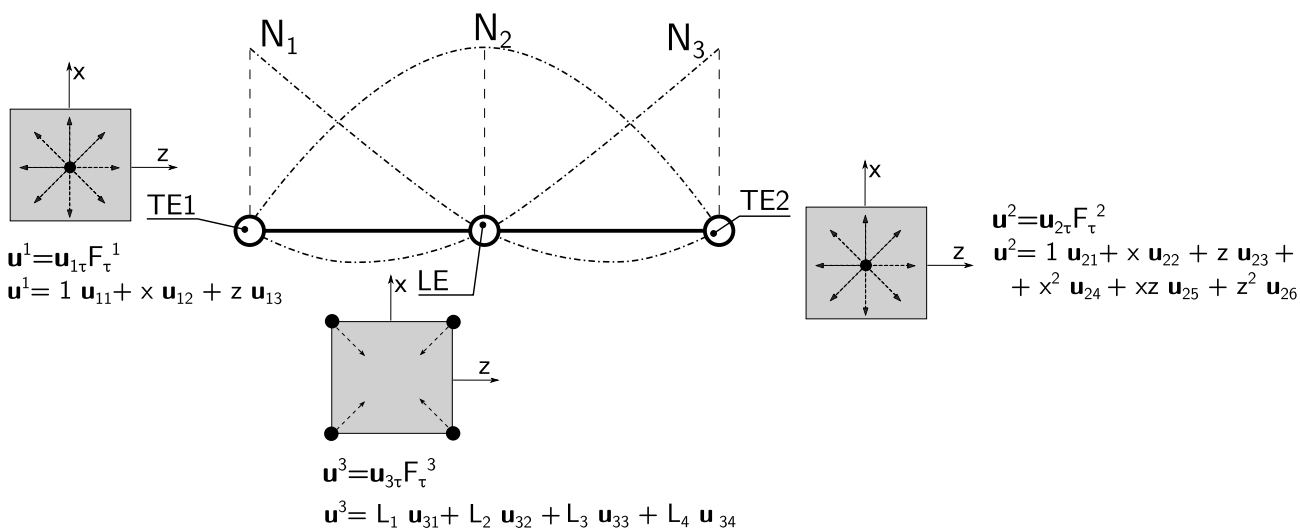

Figure 4. A three-node one-dimensional element with node-dependent kinematics.

$$\delta L_{ine} = \int_V \rho \delta \boldsymbol{q}^T \ddot{\boldsymbol{q}} dV \tag{22}$$

where $\boldsymbol{q}$ are the general displacement unknowns, $\ddot{\boldsymbol{q}} = \{\ddot{u}_x, \ddot{u}_y, \ddot{u}_z, 0\}^T$ are the accelerations, and ρ the material density. By substituting the FE discretization expression, Equation 28, into Equation 22, the following equation can be attained:

$$\delta L_{ine} = \delta \boldsymbol{q}_{js}^T \int_V \rho N_i F_s^j N_j F_\tau^i \boldsymbol{I} dV \ddot{\boldsymbol{q}}_{i\tau} = \delta \boldsymbol{q}_{js}^T \boldsymbol{m}_{ij\tau s} \ddot{\boldsymbol{q}}_{i\tau} \tag{23}$$

where $\boldsymbol{I}$ is a 3×3 identity matrix, and $\boldsymbol{m}_{ij\tau s}$ is the FN for the mass matrix which contains four sub-matrices as follows:

$$\boldsymbol{m}_{ij\tau s} = \begin{bmatrix} \boldsymbol{m}^{uu} & \boldsymbol{0} \\ \boldsymbol{0} & 0 \end{bmatrix}_{ij\tau s} \tag{24}$$

Thus, for a system without damping, the governing equations can be obtained as:

$$\boldsymbol{M}\ddot{\boldsymbol{U}} + \boldsymbol{K}\boldsymbol{U} = F \tag{25}$$

where $\boldsymbol{M}$ and $\boldsymbol{K}$ are the global mass and stiffness matrices assembled as shown in Carrera et al. (2014) starting from the fundamental nuclei. $\boldsymbol{U}$ is the vector of the nodal displacements. If the harmonic solutions are introduced, natural frequencies can be obtained by solving the following eigenvalue problem:

$$(\boldsymbol{M} - \frac{1}{\omega^2}\boldsymbol{K})\boldsymbol{U} = 0 \tag{26}$$

Otherwise, the frequency response due to a harmonic load can be evaluated solving the following equation within the range of interest of ω:

$$-\boldsymbol{M}\omega^2 + \boldsymbol{K} = F\omega \tag{27}$$

Node-dependent kinematic elements for smart structures with piezo-patches

The analysis of beam structures with piezo-patches require models able to deal complex responses. Figure 5 shows an example of a beam with two piezo-patches. To obtain accurate solutions a computational model has to describe in detail the interface between the structure and the patch. Piezo-materials usually show different mechanical and piezo-mechanical properties in different directions, that is models must be able to include the effects due to the orthotropic materials. Finally, complex displacements field must be described, that is, a three-dimensional solution is required.

All these difficulties in the analysis of piezoelectric beams are well known in literature as shown by the reviews presented by (Kapuria et al. 2010) and (Benjeddou 2000).

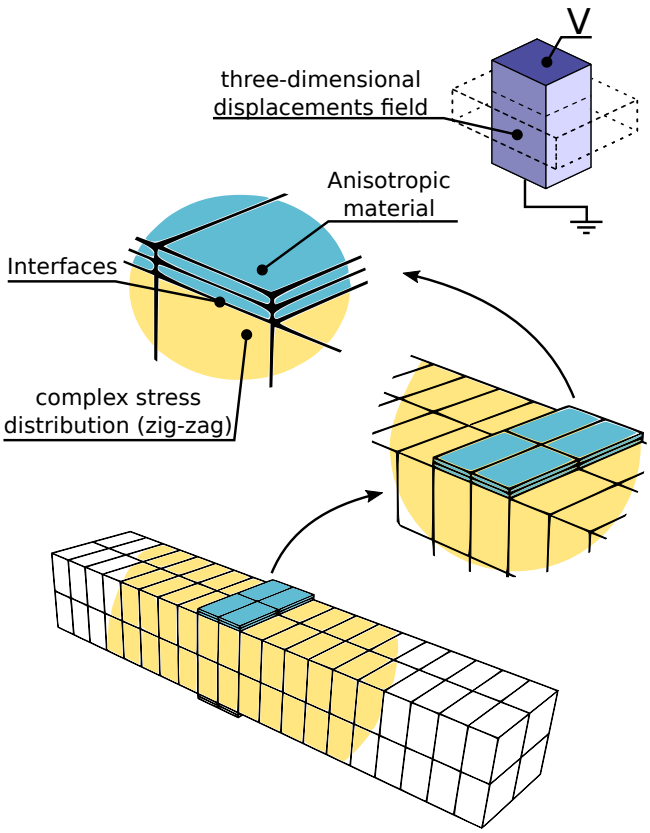

Figure 5. Example of a structure with piezo-patches.

In many cases accurate results can be only obtained using three-dimensional models that have no assumptions on the kinematic model but require a huge computational cost.

When structures with piezo-patches have to be investigated refined models are only required in the are where the patches are applied. The use of a refined model over the whole structural domain requires more computational costs than those necessary. The best solution would be to use refined models only in the region in which they are required and classical models elsewhere. The problem of mixing or joining different structural models is a well-known topic in literature. One example is the work proposed by Kim et al. (1997) where a hybrid two-/three-dimensional element has been used. In this case a classic plate element is connected to a three-dimensional element used in the area where a piezo-patch is applied. Another example is the model proposed by Biscani et al. (2012) that uses the Arlequin method to couple higher and lower order plate models, in this way refined models are used only in the piezo-patch area.

The present paper presents a new modeling approach that makes it possible to use a different kinematic approximation at each node of a finite element.

Figure 6 shows an example of a beam with piezo-patches modeled using the node-dependent kinematic approach. The piezo-patches can be included in the model considering a beam with a variable cross-section, as introduced by Carrera et al. (2013). Figure 6 shows how two section with different shape can be connected in case the shared node uses a LE model. The elements in which is present the piezo-patch can be studied using a Layer-wise, e.g. an LE model, able to capture the details of the interface between the layers. A lower order beam model can be used elsewhere. The transition from a lower to a higher kinematic approximation is done using the node dependent kinematic elements able to have different kinematics at different nodes.

Numerical results

Two beam structures with piezo-patches have been considered in this section. The first example has been used to assess the present model and the results have been compared with those from the work by Chevallier et al. (2008). The free vibrations of both short and close circuit configurations have been investigated and the electro-mechanical coupling coefficient, *EMCC*, has been used to compare the results with those from literature. The second example considers the piezo-patched beam investigated in the works by Benjeddou et al. (1997) and Carrera et al. (2017c). In this case the free vibration and the frequency response of the beam, using the piezo-patches as sensors, have been considered.

Assessment of the piezo-mechanical model with node-dependent kinematic

The present one-dimensional model with node-dependent kinematics has been assessed in this section. The benchmark proposed by Chevallier et al. (2008) has been considered. Figure 7 shows the geometry, the boundary conditions and the FE discretization. The beam is built in

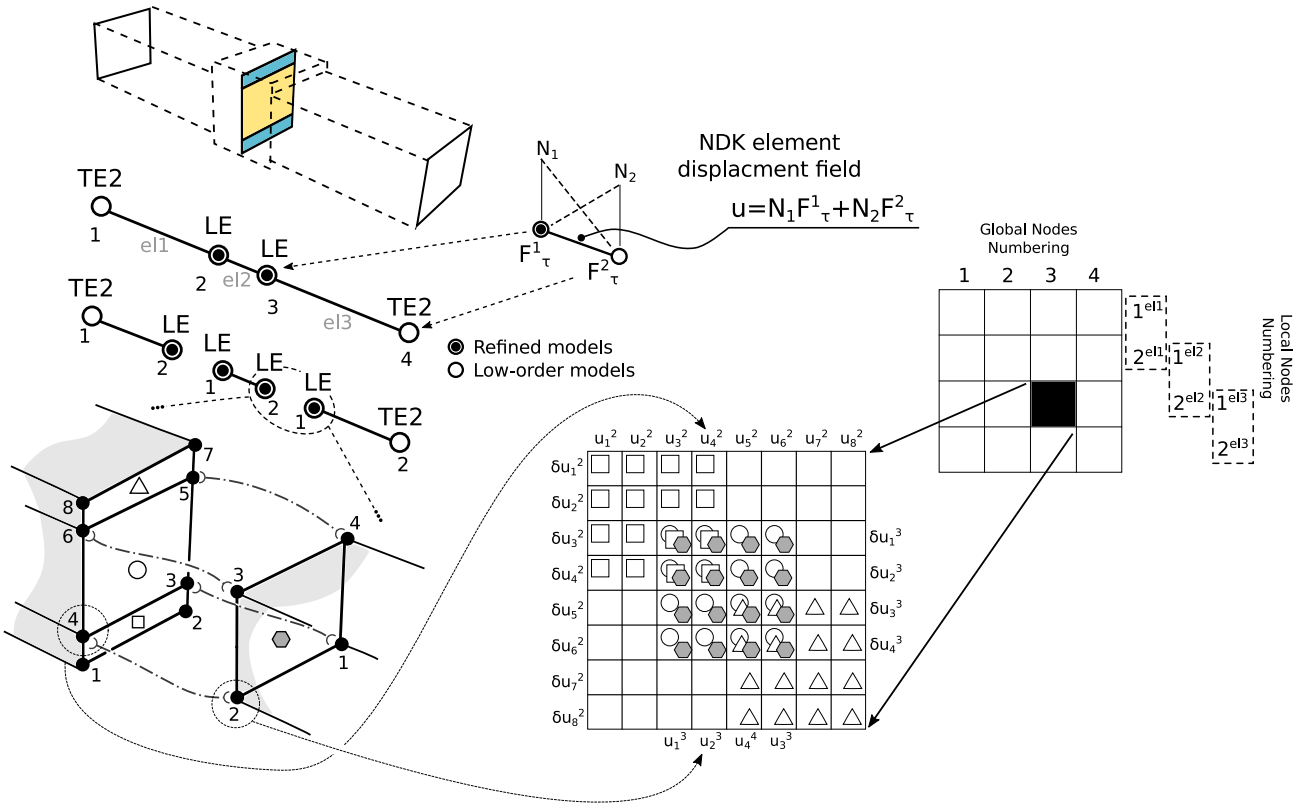

Figure 6. An example of a beam with piezo-patches modeled using the node-dependent kinematic approach.

aluminum which has the Young's modulus $E = 69\ GPa$ and Poisson's ratio $\nu = 0.3$. The aluminum density has been considered equal to $2700\ Kg/m^3$. The piezoelectric material has been considered to be the $PIC255$ material, the properties can be found in Chevallier et al. (2008). Two different sets ofboundary conditions have been considered for the piezo-patches. In the first case the emphShort circuit configuration has been considered, that is, a null potential has been imposed at the top and at the bottom of the piezoelectric patches. The *Open circuit* configuration has been considered in the second case when a null potential has been imposed only at the interface between the patches and the beam while an equipotential surface has been imposed at the external surface of the patches. This condition reproduces the presence of an electrode. Two models have been considered. The first is a one-dimensional model in which all the nodes use a Lagrange based expansion, *LE model*. The second model uses the Lagrange expansion only in the area of the patches while a Taylor expansion of the third and first order has been used elsewhere, this model has been named *LE-TE model*. The results have been compared with those proposed in the work by Chevallier et al. (2008) obtained using a solid model with 1700 elements and 9667 nodes. Assuming 3 degrees of freedom at each node (valid for the mechanical problem) a total amount of 29001 degrees of freedom has been considered for this model. Tables 1 and 2 report the first four natural frequencies evaluated for the short and open circuit configuration respectively. In both cases it is clear that the *LE model* is able to predict the dynamic

	Short circuit		
	LE model	LE-TE model	Chevallier et al. (2008)
DOFs	9170	7950	29001^M
1	$493.28^{\ 0.04\%}$	$494.29^{\ 0.25\%}$	493.07
2	$2803.1^{\ 0.19\%}$	$2804.7^{\ 0.24\%}$	2797.9
3	$3112.0^{\ 2.23\%}$	$3157.6^{\ 3.73\%}$	3044.1
4	$3247.2^{\ -0.06\%}$	$3257.9^{\ 0.27\%}$	3249.0

Table 1. First four natural frequencies for the Short circuit case. The percentage difference with respect to the reference has been reported in apex. The ^{M} notation means that the value of the DOFs is evaluated for the pure mechanical problem.

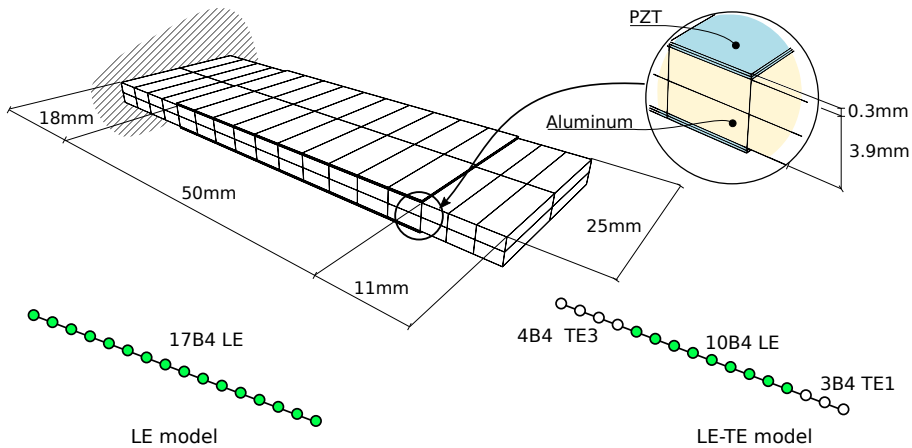

Figure 7. Geometry, boundary conditions and FE discretization of the beam with piezo-patches.

	Open circuit		
	LE model	LE-TE model	Chevallier et al. (2008)
DOFs	9170	7950	29001^M
1	$496.61^{\,0.20\%}$	$496.72^{\,0.22\%}$	495.61
2	$2803.1^{\,0.19\%}$	$2804.7^{\,0.24\%}$	2797.9
3	$3112.0^{\,2.23\%}$	$3157.6^{\,3.73\%}$	3044.1
4	$3311.2^{\,-0.17\%}$	$3326.2^{\,0.28\%}$	3317.0

Table 2. First four natural frequencies for the Open circuit case. The percentage difference with respect to the reference has been reported in apex. The ^{M} notation means that the value of the DOFs is evaluated for the pure mechanical problem.

behavior of the structure with an accuracy comparable with the reference model using one third of the degrees of freedom. The introduction of the node-dependent kinematic model allows the computational cost to be further reduced using a layer-wise model only where the piezo-patches are applied. Figures 8a-d show the first four modal shapes evaluated using the *LE model*. Modes 1 and 4 are transversal bending modes, the displacement field field suggests that the patches will be prone to compression or traction, that is an electric field can appear during the deformation. Mode 2 is a lateral bending mode while mode 3 is a torsional mode. The presence of the equipotential surface, coupled with the displacement field, does not allow any voltage to appear. This behavior can be studied introducing the *electro mechanical coupling coefficient*, K, that provide an estimation of the mechanical energy converted into electric potential energy. This coefficient can be evaluated, in according with Chevallier et al. (2008), as follow:

$$K^2 \approx \frac{\omega_{OC}^2 - \omega_{SC}^2}{\omega_{SC}^2} \tag{28}$$

where ω_{OC} and ω_{SC} are the frequency evaluated considering the open and short circuit respectively. Table 3 shows the electro mechanical coupling coefficients evaluated for each frequency using the models presented in this work. The results confirm that frequencies 3 and 4 have a K^2 higher than zero, that is, part of the mechanical energy is transformed into electric potential energy during the vibration. Modes 2 and 3 have a K^2 null, that is these modes do not produce any electric potential energy. The results obtained with the present models are in according with those from literature. In conclusion the present models can be considered reliable and accurate, the use of the node-dependent kinematics elements lead to a reduction in the computational costs. The advantages of the node-dependent kinematic models may be more evident when the piezo-patches involve only a limited part of the whole structure as in the case shown in the next section.

Dynamic analysis of a beam with piezo-patches

A prismatic beam with two piezo-patches has been considered in this section. The geometry of the model has been inspired by the work proposed by Benjeddou et al. (1997) and Carrera et al. (2017c) where the static response of the same beam has been investigated. The beam has a

	K^2			K		
	LE model	LE-TE model	Chevallier et al. (2008)	LE model	LE-TE model	Chevallier et al. (2008)
1	1.35	0.99	1.03	11.6	9.93	10.2
2	0.00	0.00	0.00	0.00	0.00	0.00
3	0.00	0.00	0.00	0.00	0.00	0.00
4	3.98	4.24	4.27	19.9	20.6	20.7

Table 3. Electro mechanical coupling coefficients evaluated using the *LE model* and the *LE-TE model*.

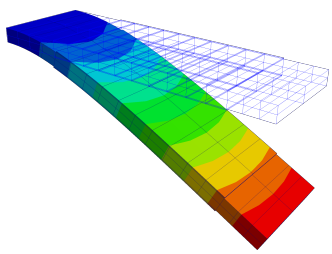

(a) Mode 1, 493.28 Hz.

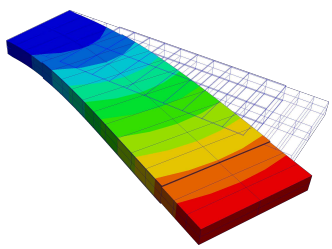

(b) Mode 2, 2803.1 Hz.

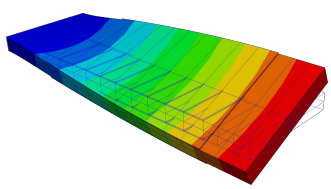

(c) Mode 3, 3112.0 Hz.

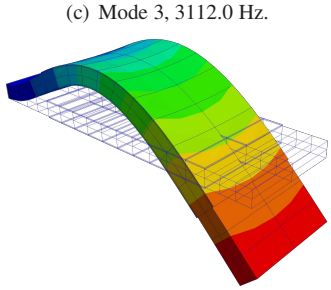

(d) Mode 4, 3247.2 Hz.

Figure 8. First four modes evaluated using the *LE model* for the short circuit case.

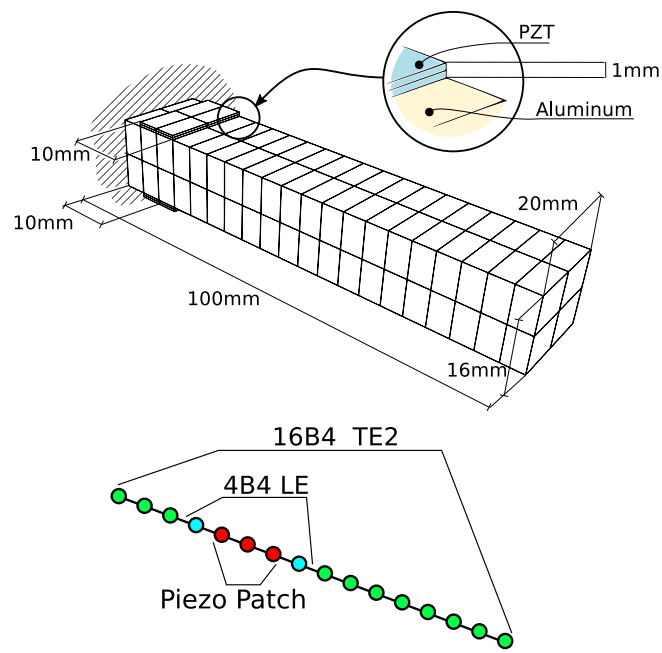

Figure 9. Geometry, boundary conditions and FE discretization of the beam with short piezo-patches.

compact square cross-section and two piezo-patches have been placed close to the clamped end. The geometry of the model has been shown in Figure 9. The piezoelectric patches are made of PZT-5H, whose material coefficients have been listed in Table 4, and the substrate structures employ aluminum which has the Young's modulus $E = 70.3$GPa and Poisson's ratio $\nu = 0.345$.

Two models have been considered. The first uses the same kinematic, based on the Lagrange expansion, along the whole beam, *LE model*. The second uses a LE kinematic only where the patches are placed while a second order Taylor model is used elsewhere. This model is referred as *LE-TE2 model*. The FE discretization has been shown in Figure 9. The accuracy of these models for the static analysis has been assessed by Carrera et al. (2017c), in this work the capabilities of the resent approach in the analysis of local stress fields due to material discontinuities have been investigated.

At first a free vibration analysis has been performed. Table 5 reports the first ten natural frequencies evaluated

Table 4. Material properties of PZT-5H

C_{11},C_{22},C_{33} [GPa]	C_{12} [GPa]	C_{13},C_{23} [GPa]	C_{44},C_{55},C_{66} [GPa]	e_{15},e_{24} [C/m^2]	e_{31},e_{32} [C/m^2]	e_{33} [C/m^2]	χ_{11},χ_{22} [F/m]	χ_{33} [F/m]
126	79.5	84.1	23.0	17.0	-6.5	23.3	1.503×10^{-8}	1.30×10^{-8}

	LE model	LE-TE2 model	
DOFs	5765	3317	-42.46%
1	1363.1	1362.1	-0.07%
2	1637.2	1639.5	0.14%
3	7214.3	7495.1	3.89%
4	7460.0	7586.1	1.69%
5	8744.9	8808.4	0.73%
6	12941.5	12936.1	-0.04%
7	18080.8	18239.2	0.88%
8	20658.1	20885.4	1.10%
9	21308.1	22464.5	5.43%
10	30697.3	31146.8	1.46%

Table 5. First ten Frequencies of the piezo-patched beam.

using the constant and the node-dependent kinematics models respectively. The *LE-model* is considered as a reference. The results show that the use of a node-dependent kinematic model can lead to accurate results. In this case the 9th frequency show an error of 5.4% and the 3rd an error of 3.9% while all the other frequencies show errors lower than 2%. At the same time the use of the *LE-TE2 model* ensures a reduction of the computational cost of the 42%.

Figures 10a-f show the first six modal shapes evaluated by means of the *LE-TE2 model*. In this case flexural, torsional and axial modes can be observed.

The accuracy of the refined kinematic models can be appreciated looking at the stress fields related to the natural modes. Figure 11 shows the axial stress evaluated in the piezo patch. The results show that LE such as TE2/LE models can predict a stress distribution comparable with the 3D solution (HEXA 27 elements, 31428 DOFs). The TE2 model fail in the prediction of the boundary conditions in fact, due to the force equilibrium, at y=0.005 and y=0.015 the axial stress should go to zero. Figure 11 reports the dimensional through-the-thickness distribution of the axial stress and the voltage due to the first natural mode. It can be seen that the axial stress evaluated using Lagrange based models can predict the 3D solution. The voltage distribution has a step-wise behavior that can not be predicted using a TE2 model because the null voltage in the metallic beam acts as a constrain also in the piezo-patches leading to a wrong result. The use of a LE models allow to predict the correct distribution of the potential.

In order to verify which of them is able to convert mechanical energy into electrical potential energy a frequency response analysis has been performed. A harmonic force F of components [1,1,1] has been applied at the top right corner of the tip cross-section in order to excite all the modes of the structure. Figure 13 shows the frequency response of the structure. The dashed line shows the frequency response, evaluated using the *LE-TE2 model*, of the structure in term of displacement magnitude amplification at the tip. The points represent the same frequency response evaluated using the *LE model*. From these results it is clear that the node-dependent kinematics model is able to reproduce perfectly the dynamic behavior of the model with a constant, refined, kinematic. The solid line shows the voltage amplification evaluated in one of the piezo-patches. The results show that the voltage is strongly amplified in correspondence of some resonances, e.g. the first and the third peaks that are related to the first and the third modes. Others mechanical resonances, e.g. the second, does not affect the electric response. This means that the actual patches configuration cannot be used to detect some modes if the patches are used as sensor. On the other side, not all the modes are able to create a voltage in the patches, that is, it is not possible to extract electric potential energy from these modes for energy harvesting applications.

In the bottom left part of Figure 13 are reported the comparisons between the two models in terms of degrees of freedom and solution time. It is clear that the use of the node-dependent kinematics approach can led to a strong reduction in the computational time. The computational efficiency becomes very important when the same problem

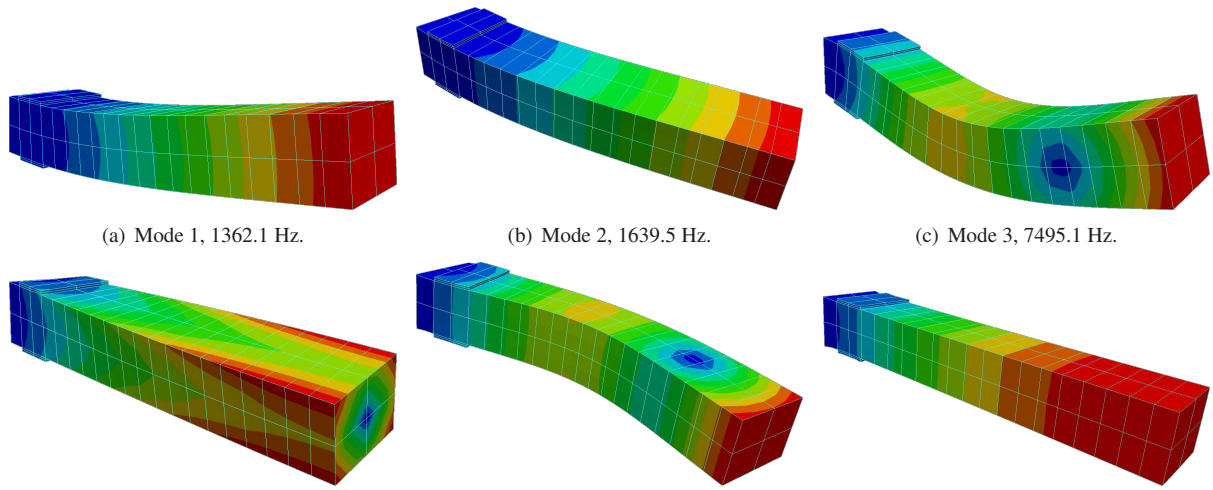

(a) Mode 1, 1362.1 Hz. (b) Mode 2, 1639.5 Hz. (c) Mode 3, 7495.1 Hz.

(d) Mode 4, 7586.1 Hz. (e) Mode 5, 8808.4 Hz. (f) Mode 6, 12936.1 Hz.

Figure 10. First six modes evaluated using the *LE-TE2 model*.

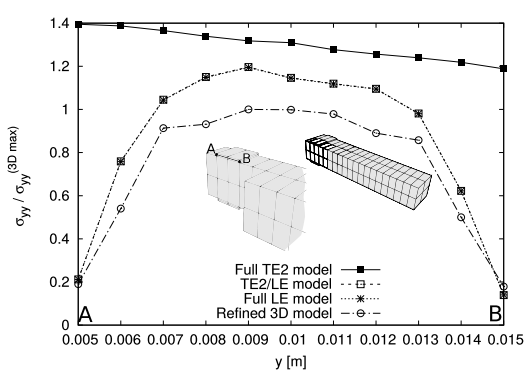

Figure 11. Axial stress distribution in the piezo-patch. The values have been normalized using the maximum stress evaluated using the 3D model.

has to be solved many times as in the case of the frequency response analysis.

Conclusions

The present work exhibits the use of FE models with node-dependent kinematics (NDK) to the dynamic analysis of beams with piezo-patches. Derived from Carrera Unified Formulation (CUF), the governing equations of the present NDK FE modes can be derived in a compact and generic manner. Through NDK, an adaptive kinematic refinement can be carried out on the nodal level in the desired structural region. This approach can be applied in the construction of FE models with variable LW/ESL nodal capabilities. Through NDK, refined kinematics models can only be used in the patched area while low order models can be used elsewhere. This approach allows the computational costs to be reduced without a reduction in the results accuracy. Based on the numerical investigation, the following conclusions can be drawn:

- The NDK based on CUF proves to be a practical approach to define the local kinematic refinement at arbitrary desired nodes in an FE model without using *ad hoc* coupling.
- The use of refined kinematic one-dimensional models in the piezo-patches areas makes it possible to obtain a *quasi 3D* solution and to impose complex boundary conditions;
- By means of the LW models employed in the local region contains the piezo-patches, the different constitutive relations in the piezoelectric and structural components can be properly addressed;
- The utilization of lower order ESL kinematics in the outlying zone allows the computational cost to be reduced;
- Taking advantage of the convenience in defining local refinement of NDK, the segmented distribution of the piezo-patches can be appropriately captured with one-dimensional elements.

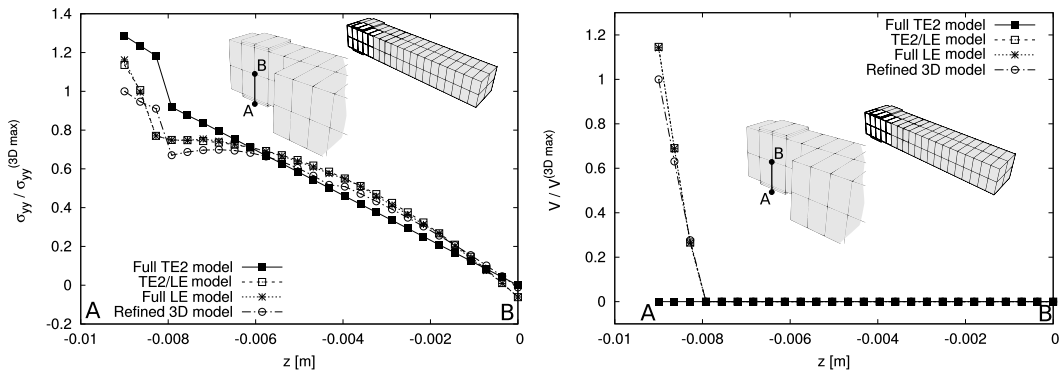

(a) Axial stress distribution. (b) Voltage distribution.

Figure 12. Through-the-thickness distribution of the axial stress and the voltage. The values have been normalized using the maximum stress evaluated using the 3D model.

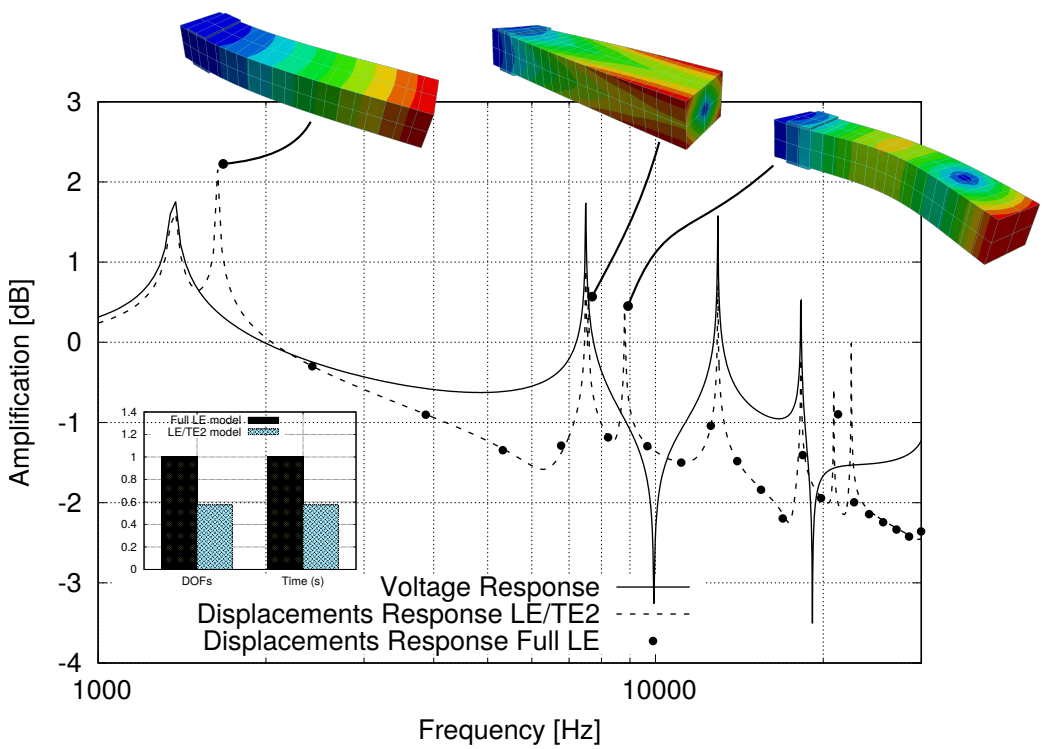

Figure 13. Frequency response of the beam structure with piezo-patches.

As demonstrated by the outcomes of this research, the use of NDK models represent an optimum compromise between accuracy and computational consumption. The efficiency of these models can be exploited to speed-up the solution time especially when iterative solution are required. The present models can be applied to the design of vibration control devices and energy harvesting applications.

Acknowledgements

This research work has been carried out within the project FULLCOMP (FULLy analysis, design, manufacturing, and health monitoring of COMPosite structures), funded by the European Union Horizon 2020 Research and Innovation program under the Marie Skłodowska Curie grant agreement No. 642121.

References

Allik H and Hughes TJ (1970) Finite element method for piezoelectric vibration. *International journal for numerical methods in engineering* 2(2): 151–157.

Batra R (1995) Deflection control during dynamic deformations of a rectangular plate using piezoceramic elements. *AIAA Journal* 33(8): 1547–1548.

Batra R and Liang X (1997) Finite dynamic deformations of smart structures. *Computational mechanics* 20(5): 427–438.

Benjeddou A (2000) Advances in piezoelectric finite element modeling of adaptive structural elements: a survey. *Computers & Structures* 76(1): 347–363.

Benjeddou A, Trindade M and Ohayon R (1997) A unified beam finite element model for extension and shear piezoelectric actuation mechanisms. *Journal of Intelligent Material Systems and Structures* 8(12): 1012–1025.

Biscani F, Nali P, Belouettar S and Carrera E (2012) Coupling of hierarchical piezoelectric plate finite elements via Arlequin method. *Journal of Intelligent Material Systems and Structures* 23(7): 749–764. DOI:10.1177/1045389X12437885.

Carrera E (2002) Theories and finite elements for multilayered, anisotropic, composite plates and shells. *Archives of Computational Methods in Engineering* 9(2): 87–140.

Carrera E, Brischetto S and Nali P (2011) *Plates and shells for smart structures: classical and advanced theories for modeling and analysis*, volume 36. John Wiley & Sons.

Carrera E, Cinefra M, Li G and Kulikov G (2016) MITC9 shell finite elements with miscellaneous through-the-thickness functions for the analysis of laminated structures. *Composite Structures* 154: 360–373.

Carrera E, Cinefra M, Petrolo M and Zappino E (2014) *Finite element analysis of structures through Unified Formulation*. John Wiley & Sons.

Carrera E, Giunta G, Nali P and Petrolo M (2010) Refined beam elements with arbitrary cross-section geometries. *Computers & Structures* 88(5-6): 283–293. DOI:10.1016/j.compstruc.2009.11.002.

Carrera E, Pagani A and Valvano S (2017a) Multilayered plate elements accounting for refined theories and node-dependent kinematics. *Composites Part B: Engineering* 114: 189–210.

Carrera E and Petrolo M (2012) Refined Beam Elements with only Displacement Variables and Plate/Shell Capabilities. *Meccanica* 47(3): 537–556. DOI:10.1007/s11012-011-9466-5.

Carrera E, Petrolo M and Zappino E (2012) Performance of CUF approach to analyze the structural behaviour of slender bodies. *Journal of Structural Engineering* 138(2): 285–297. DOI:10.1061/(ASCE)ST.1943-541X.0000402.

Carrera E, Valvano S and Kulikov GM (2017b) Multilayered plate elements with node-dependent kinematics for electromechanical problems. *International Journal of Smart and Nano Materials* 0(0): 1–39. DOI:10.1080/19475411.2017.1376722.

Carrera E and Zappino E (2017) One-dimensional finite element formulation with node-dependent kinematics. *Computers & Structures* 192: 114–125.

Carrera E, Zappino E and Li G (2017c) Analysis of beams with piezo-patches by node-dependent kinematic finite element method models. *Journal of Intelligent Material Systems and Structures* 0(0): 1045389X17733332. DOI:10.1177/1045389X17733332.

Carrera E, Zappino E and Li G (2018) Finite element models with node-dependent kinematics for the analysis of composite beam structures. *Composites Part B: Engineering* 132(Supplement C): 35 – 48.

Carrera E, Zappino E and Petrolo M (2013) Analysis of thin-walled structures with longitudinal and transversal stiffeners. *Journal of Applied Mechanics* 80(1): 11006–11012. DOI:10.1115/1.4006939.

Chevallier G, Ghorbel S and Benjeddou A (2008) A benchmark for free vibration and effective coupling of thick piezoelectric smart structures. *Smart Materials and Structures* 17(6): 065007.

Cinefra M, Lamberti A, Zenkour AM and Carrera E (2015) Axiomatic/asymptotic technique applied to refined theories for piezoelectric plates. *Mechanics of Advanced Materials and Structures* 22(1-2): 107–124.

Heyliger P, Ramirez G and Saravanos D (1994) Coupled discrete-layer finite elements for laminated piezoelectric platess. *International Journal for Numerical Methods in Biomedical Engineering* 10(12): 971–981.

Huang JH and Wu TL (1996) Analysis of hybrid multilayered piezoelectric plates. *International Journal of Engineering*

Science 34(2): 171–181.

Jonnalagadda K, Blandford G and Tauchert T (1994) Piezothermoelastic composite plate analysis using first-order shear deformation theory. *Computers & Structures* 51(1): 79–89.

Kapuria S (2001) An efficient coupled theory for multilayered beams with embedded piezoelectric sensory and active layers. *International Journal of Solids and Structures* 38(50): 9179–9199.

Kapuria S (2004) A coupled zig-zag third-order theory for piezoelectric hybrid cross-ply plates. *Transactions, American Society of Mechanical Engineers* 71(5): 604–614.

Kapuria S and Hagedorn P (2007) Unified efficient layerwise theory for smart beams with segmented extension/shear mode, piezoelectric actuators and sensors. *Journal of Mechanics of Materials and Structures* 2(7): 1267–1298.

Kapuria S, Kumari P and Nath JK (2010) Efficient modeling of smart piezoelectric composite laminates: a review. *Acta Mechanica* 214(1-2): 31–48.

Kim J, Varadan VV and Varadan VK (1997) Finite element modelling of structures including piezoelectric active devices. *International Journal for Numerical Methods in Engineering* 40(5): 817–832.

Kpeky F, Abed-Meraim F, Boudaoud H and Daya EM (2017) Linear and quadratic solidshell finite elements SHB8PSE and SHB20E for the modeling of piezoelectric sandwich structures. *Mechanics of Advanced Materials and Structures* DOI:10.1080/15376494.2017.1285466. In press.

Lee C (1990) Theory of laminated piezoelectric plates for the design of distributed sensors/actuators. Part I: Governing equations and reciprocal relationships. *The Journal of the Acoustical Society of America* 87(3): 1144–1158.

Mackerle J (2003) Smart materials and structuresa finite element approachan addendum: a bibliography (1997–2002). *Modelling and Simulation in Materials Science and Engineering* 11(5): 707.

Miglioretti F, Carrera E and Petrolo M (2014) Variable kinematic beam elements for electro-mechanical analysis. *Smart Structures and Systems* 13(4): 517–546.

Mitchell J and Reddy J (1995) A refined hybrid plate theory for composite laminates with piezoelectric laminae. *International Journal of Solids and Structures* 32(16): 2345–2367.

Robbins D and Reddy J (1991) Analysis of piezoelectrically actuated beams using a layer-wise displacement theory. *Computers & Structures* 41(2): 265–279.

Trindade MA and Benjeddou A (2009) Effective electromechanical coupling coefficients of piezoelectric adaptive structures: critical evaluation and optimization. *Mechanics of Advanced Materials and Structures* 16(3): 210–223.

Wang BT and Rogers CA (1991) Laminate plate theory for spatially distributed induced strain actuators. *Journal of Composite Materials* 25(4): 433–452.

Washizu K (1968) *Variational methods in elasticity and plasticity*. Oxford: Pergamon Press.

Zappino E, Carrera E, Rowe S, Mangeot C and Marques H (2016a) Numerical analyses of piezoceramic actuators for high temperature applications. *Composite Structures* 151: 36–46.

Zappino E, Cavallo T and Carrera E (2016b) Free vibration analysis of reinforced thin-walled plates and shells through various finite element models. *Mechanics of Advanced Materials and Structures* 23(9): 1005–1018. DOI:10.1080/15376494.2015.1121562.

Zappino E, Li G, Pagani A and Carrera E (2017) Global-local analysis of laminated plates by node-dependent kinematic finite elements with variable ESL/LW capabilities. *Composite Structures* 172: 1–14.